MOTIF: Evaluation of time spectra for nuclear forward scattering

Yuri V. Shvyd'ko

II. Institut für Experimentalphysik, Universität Hamburg, D-22761 Hamburg, Germany
E-mail: yuri.shvydko@desy.de

The computer program MOTIF calculates time dependences for nuclear forward scattering (NFS) of synchrotron radiation and allows fully automatic fits of experimental data. A multiple scattering technique of calculations directly in space and time is used. The source code of MOTIF is written in Fortran 77. It has been worked out since 1993 and tested on several Unix platforms by fitting the NFS time spectra of ^{57}Fe, ^{119}Sn, ^{151}Eu, ^{161}Dy, and ^{181}Ta nuclei in various compounds with different time-independent and time-dependent hyperfine interactions.

Keywords: nuclear resonance, X-rays, coherent scattering, time dependence

1. Introduction

Time spectroscopy of nuclear resonant scattering by using synchrotron radiation as a source was introduced by Gerdau et al. [1] in Bragg diffraction experiments using YIG single crystals. The outstanding features of the source, such as high brilliance, high degree of polarization, pulse structure, and practically zero width of the radiation pulse in time, define its great potential. With the advent of meV-monochromators experiments in forward scattering geometry with synchrotron radiation and, in particular, measurements of nuclear forward scattering (NFS) time spectra became feasible [2]. NFS opens many new possibilities as it is not limited to single crystal samples. The advent of the meV-monochromators also made feasible time spectroscopy at grazing incidence [3], and small-angle scattering [4].

Bragg, forward, small-angle, and grazing incidence scattering processes are spatially coherent. Therefore, interference effects play a significant role, providing, in general, more physical information about the samples, making, however, the "reading" of the time spectra also more complicated. Generally speaking, the time spectra of nuclear resonant scattering are not as evident as their counterpart, the energy spectra. Even the qualitative interpretation of the time spectra, perhaps with the exception of the single-resonance case, is practically impossible without computer calculations. Availability of computer programs for the evaluation and interpretation of the experimental time spectra as well as for theoretical modelling is absolutely necessary. The

© J.C. Baltzer AG, Science Publishers

computer program may even be so powerful as allowing not only to fit the data but also to simulate experiments.

MOTIF is one such program destined for the evaluation of NFS time spectra. MOTIF calculates time spectra for NFS of synchrotron radiation in thin and thick samples with polarization mixing and provides, if required, automatic fits to experimental spectra. The source code of MOTIF is written in Fortran 77. It has been worked out since 1993 and tested on different Unix platforms like LINUX, IRIX, AIX, etc., by fitting the NFS time spectra of ^{57}Fe, ^{119}Sn, ^{151}Eu, ^{161}Dy, and ^{181}Ta nuclei in different compounds with different hyperfine interactions.

One of the distinguishing features of MOTIF is its technique of calculation, which is performed directly in time and space [5]. It does not require the initial knowledge of the corresponding frequency spectral function of NFS, which is necessary in the more widespread frequency–time Fourier transformation technique [6–11]. Clearly, both direct and Fourier transformation techniques applied to the same problems should give the same results. The direct procedure implemented in MOTIF is attractive in cases where the calculation of the NFS frequency spectral function of the scatterer is not straightforward. Actually, this task is relatively simple only for problems with time-independent hyperfine interactions, or for problems which can be formally reduced to them, like some models of diffusion. In all other cases, which include dynamics, e.g., time-dependent motion of nuclei (thermal vibrations, diffusion, external perturbations) or time-dependent hyperfine interactions (relaxation phenomena, external perturbations), the NFS frequency spectrum cannot be calculated directly.

Generally speaking, with the Fourier transformation technique three preparatory calculation steps are required, as described below. As a result the calculation of the time spectrum together with the frequency–time, Fourier transformation requires four calculation steps. In the first step the nuclear double-time self-correlation function $K^{s\tilde{s}}(t,\tilde{t})$ should be calculated. $K^{s\tilde{s}}(t,\tilde{t})$ describes the time dependence of the single-scattering coherent response of the nuclear system in the forward direction at time t to the excitation at time $\tilde{t}$ [5]. The upper indices $\tilde{s}$ and s denote orthogonal polarization components of the incident and scattered radiation. $K^{s\tilde{s}}(t,\tilde{t})$ reflects coherent scattering properties of a single nucleus and bears information on the spatial motions of nuclei and nuclear hyperfine interactions averaged over the whole nuclear ensemble. In the second step the double-frequency Fourier image $K^{s\tilde{s}}(\omega,\widetilde{\omega})$ is calculated. The ω-dependence in $K^{s\tilde{s}}(\omega,\widetilde{\omega})$ gives the frequency spectrum of NFS in the single-scattering approximation of the nuclear system exposed to the incident monochromatic radiation of frequency $\widetilde{\omega}$. In the third step, the optical multiple scattering problem is solved for the given $K^{s\tilde{s}}(\omega,\widetilde{\omega})$ in the frequency domain by using the classical Maxwell wave equations or the equations of quantum electrodynamics, which leads to the NFS frequency spectrum $S^{s\tilde{s}}(\omega,\widetilde{\omega})$. Only in the fourth step the time spectrum of NFS is calculated from $S^{s\tilde{s}}(\omega,\widetilde{\omega})$ by using the double frequency–time Fourier transformation for the given frequency spectrum of the incident radiation.

By contrast, in the direct procedure implemented in MOTIF the first step, i.e., the calculation of the nuclear double-time self-correlation function $K^{s\tilde{s}}(t,\tilde{t})$ is followed

by only one more step of solving the optical multiple scattering problem directly in time and space, which results in the desired time spectrum of NFS. This procedure is independent of the particular form of $K^{s\tilde{s}}(t,\tilde{t}\,)$ and is based on the general multiple scattering solution of the NFS wave equation with $K^{s\tilde{s}}(t,\tilde{t}\,)$ as its kernel. The derivation of the NFS wave equation, its multiple scattering solution, and examples of the nuclear self-correlation functions for particular cases of spatial motions and hyperfine interactions are given in [5] and are briefly outlined in section 2.

This paper describes how this procedure implemented in MOTIF works in particular cases of hyperfine interactions and nuclear spatial motions. Cases presented are: time-independent hyperfine interactions – section 3.1, time-dependent hyperfine interactions due to switching of the magnetic hyperfine field – section 3.2. In sections 3.3 and 3.4, suggestions are made, how to apply MOTIF for the evaluation of time spectra affected by diffusion of atoms and the atomic spin relaxation is suggested.

2. Theoretical background

The time spectrum $S(t)$ of NFS is proportional to the square modulus of the vector amplitude $\boldsymbol{E}(L,t)$ of the coherent radiation field which emerges from the back of the sample in the direction of the primary beam:

$$S(t) \propto \left|\boldsymbol{E}(L,t)\right|^2 = \sum_s \left|E^s(L,t)\right|^2. \tag{2.1}$$

The upper index s corresponds to any of two orthogonal polarization components of the radiation, given by the polarization vectors $\boldsymbol{e}^s$. L is the sample thickness.

The solution of the NFS wave equation for the vector amplitude of the radiation field $\boldsymbol{E}(L,t)$ can be presented as a power series of a dimensionless thickness parameter ξ [5]:

$$\boldsymbol{E}(L,t) = \sum_{p=0}^{\infty} \frac{(-\xi)^p}{p!}\boldsymbol{E}^{(p)}(t). \tag{2.2}$$

The quantities $\boldsymbol{E}^{(p)}(t)$ in eq. (2.2) are the multiple scattering amplitudes of order p.

The dimensionless thickness parameter $\xi = \sigma_{\mathrm{R}} N_0 L/4\gamma$ scales with the effective resonance thickness $T_{\mathrm{R}} = \sigma_{\mathrm{R}} N_0 L$[1] known from Mössbauer spectroscopy, with σ_{R} the total cross-section of the nuclear resonance absorption, N_0 is the number of resonant nuclei per unit volume, and γ is the sine of the incidence angle.

The zeroth term $\boldsymbol{E}^{(0)}(t)$ in eq. (2.2) is defined as the time dependence $\boldsymbol{\mathcal{E}}(t)$ of the incident radiation pulse:

$$\boldsymbol{E}^{(0)}(t) = \boldsymbol{\mathcal{E}}(t). \tag{2.3}$$

[1] Sometimes the Lamb–Mössbauer factor f of recoilless emission–absorption is also included in the definition of the effective thickness: $T'_{\mathrm{R}} = \sigma_{\mathrm{R}} N_0 L f$.

To describe experiments with very short synchrotron radiation pulses, $\boldsymbol{E}^{(0)}(t)$ can be taken proportional to the $\delta(t)$-function. The other terms, $\boldsymbol{E}^{(p)}(t)$, are obtained by the recursion relation

$$\boldsymbol{E}^{(p)}(t) = \frac{\Gamma_0}{\hbar} \int_{-\infty}^{t} \widehat{K}\big(t,\tilde{t}\,\big)\,\boldsymbol{E}^{(p-1)}\big(\tilde{t}\,\big)\,\mathrm{d}\tilde{t}. \tag{2.4}$$

Here $\widehat{K}(t,\tilde{t}\,)$ is a 2×2 matrix with elements $K^{s\tilde{s}}(t,\tilde{t}\,)$, which are double-time nuclear self-correlation functions. The upper indices $\tilde{s}$ and s denote orthogonal polarization components of the incident and scattered radiation, respectively. As one can see from eq. (2.4) the self-correlation function $K^{s\tilde{s}}(t,\tilde{t}\,)$ describes the coherent single-scattering response of the nuclear system in the forward direction at time t after excitation at time $\tilde{t}$.

In general, the nuclear self-correlation function is represented as

$$K^{s\tilde{s}}\big(t,\tilde{t}\,\big) = \sum_{\beta} L_{\beta}^{s\tilde{s}}\big(t,\tilde{t}\,\big)\,M_{\beta}\big(t,\tilde{t}\,\big), \tag{2.5}$$

where the summation is performed over different types β of nuclear sites in the sample [5]. Index β tags the groups of resonant nuclei possessing different interactions with the environment and (or) spatial motion. The function $M_{\beta}(t,\tilde{t}\,)$ gives information on the spatial motion of nuclei, while $L_{\beta}^{s\tilde{s}}(t,\tilde{t}\,)$ gives information on the hyperfine and intranuclear interactions of the nuclei belonging to a group β.

The correlation function has the property

$$K^{s\tilde{s}}(t,t) = \delta^{s\tilde{s}}. \tag{2.6}$$

The solution given by eqs. (2.2)–(2.4) is general and independent of the explicit form of the hyperfine interactions and nuclear spatial motion, which are hidden in the nuclear self-correlation function $K^{s\tilde{s}}(t,\tilde{t}\,)$. The self-correlation function $K^{s\tilde{s}}(t,\tilde{t}\,)$ is calculated once. To calculate the vector amplitude $\boldsymbol{E}(\xi,t)$ of the NFS time spectrum and the time spectrum (2.1) the multiple scattering procedure is applied, based on the recursion relation (2.4).

3. Examples

This section presents examples of evaluations of the NFS time spectra by using different nuclear self-correlation functions.

3.1. Time-independent hyperfine interactions

The double-time self-correlation function $K^{s\tilde{s}}(t,\tilde{t}\,)$ in the case of time-independent hyperfine interactions takes the form [5]

$$K^{s\tilde{s}}\big(t,\tilde{t}\,\big) = \mathcal{K}^{s\tilde{s}}\big(t-\tilde{t}\,\big), \tag{3.1}$$

which is typical for *elastic* coherent scattering. Only the difference $t-\tilde{t}$ between the excitation and emission times is important in this case. By virtue of this we substitute $t-\tilde{t}$ by t in the following formulae of this section. According to [5] $\mathcal{K}^{s\tilde{s}}(t)$ is given by a sum of time exponential functions:

$$\mathcal{K}^{s\tilde{s}}(t)=\eta(t)\sum_{\ell\equiv\{\beta,\beta_{\rm g},\beta_{\rm e}\}}\mathcal{A}_\ell^{s\tilde{s}}\exp\left[-\frac{\rm i}{\hbar}\left(\Omega_\ell\hbar-\frac{\rm i}{2}\Delta\Gamma_\beta\right)t\right], \tag{3.2}$$

$$\eta(t)=\exp\left\{\frac{\rm i}{\hbar}\left[\hbar\widetilde{\omega}-E_0+\frac{\rm i}{2}(\Gamma_0+\Delta\Gamma_0)\right]t\right\}\theta(t). \tag{3.3}$$

Here E_0 is the energy of the nuclear transition between the unsplit ground and the unsplit excited states, Γ_0 is the natural energy width of the nuclear excited state. The carrier frequency $\widetilde{\omega}$ of the incident radiation pulse is assumed to be close to the nuclear resonance frequency $E_0/\hbar$. To describe experiments with pulsed synchrotron radiation one can put $\widetilde{\omega}=E_0/\hbar$ without loss of generality. $\theta(t)$ is the unit step function.

Hyperfine interactions split the nuclear ground and excited states. The summation in eq. (3.2) is performed over index ℓ, which is a joint index numbering both different types of nuclear sites β in the sample and the transitions $\langle\beta_{\rm g}|\Leftrightarrow|\beta_{\rm e}\rangle$ between the ground and excited nuclear states. Here $|\beta_\lambda\rangle$ are the eigenvectors with energies $\varepsilon_{\beta_\lambda}$ of the time-independent hyperfine interaction Hamiltonian in the ground ($\lambda=$ g) or excited ($\lambda=$ e) states, respectively. Because of the splitting the nuclear transition energies become $E_0+\hbar\Omega_\ell$, where $\Omega_\ell=(\varepsilon_{\beta_{\rm e}}-\varepsilon_{\beta_{\rm g}})/\hbar$ are the frequencies entering the time exponential functions in eq. (3.2).

The amplitude

$$\mathcal{A}_\ell^{s\tilde{s}}=X_\beta f_\beta(\boldsymbol{k})j^s_{\beta_{\rm g}\beta_{\rm e}}(\boldsymbol{k})j^{\tilde{s}}_{\beta_{\rm e}\beta_{\rm g}}(-\boldsymbol{k}) \tag{3.4}$$

of the transition ℓ is proportional to the product of the absorption $j^{\tilde{s}}_{\beta_{\rm e}\beta_{\rm g}}(-\boldsymbol{k})$ and the emission $j^s_{\beta_{\rm g}\beta_{\rm e}}(\boldsymbol{k})$ matrix elements of the nuclear current density. The motional part of the self-correlation function $M_\beta(t)$ is replaced here by the time-independent Lamb–Mössbauer factors of recoilless resonant emission–absorption $f_\beta(\boldsymbol{k})$.[2] This is correct for the typical times of hyperfine interactions $t\geqslant 10^{-10}$ s; however, not in general [5]. The factor

$$X_\beta=\frac{4\widetilde{\omega}}{c^3(2J_{\rm e}+1)\Gamma_\gamma}w_\beta \tag{3.5}$$

includes the relative weight w_β of the group β, the full radiative width Γ_γ of the nuclear transition e $\Rightarrow$ g, and the nuclear spin $J_{\rm e}$ of the excited state.

MOTIF calculates $\mathcal{A}_\ell$, Ω_ℓ and the self-correlation function itself by using input parameters which define the nuclear Hamiltonian, the Lamb–Mössbauer factors, the weights of the nuclear sites, etc.

[2] As the motional part of the self-correlation function $M_\beta(t)$ is replaced here by the time-independent Lamb–Mössbauer factors, the equality $K^{s\tilde{s}}(t,\tilde{t})=\delta^{s\tilde{s}}$ is no longer valid. Instead, $K^{s\tilde{s}}(t,\tilde{t})=\delta^{s\tilde{s}}\sum_\beta f_\beta(\boldsymbol{k})w_\beta$ is applied.

MOTIF offers possibilities of taking line-broadening into account. E.g., an inhomogeneous broadening which is the same for all the nuclear transitions may be taken into account simultaneously by an additional damping constant $\Delta\Gamma_0$, as shown in eq. (3.3). Inhomogeneous broadening of the transitions due to relaxation, diffusion, etc., belonging to the nuclei in a particular group β may be described by $\Delta\Gamma_\beta$, as in eq. (3.2).

MOTIF also provides possibilities of taking into account distributions of hyperfine parameters like a distribution of magnetic hyperfine fields at the nuclear sites (see section 3.1.3 and [12]), a distribution of isomer shifts (see section 3.1.1), and a distribution of electric field gradients.

3.1.1. Single resonance, or the resolution of time domain spectroscopy

The simplest case which can be demonstrated theoretically is a single resonance. It occurs, e.g., in the absence of hyperfine interactions, i.e., when the ground and excited nuclear states are not split, and in the absence of motional broadening due to thermal motion. In this case $\beta = 1$, $\Omega_\ell = 0$, $\sum_\ell \mathcal{A}_\ell^{s\tilde{s}} = f\delta^{s\tilde{s}}$, as a result $\mathcal{K}^{s\tilde{s}}(t) = f\eta(t)\delta^{s\tilde{s}}$ and one can obtain the analytical solution for the NFS time spectrum. Speeded-up decay and dynamical-beat modulation of the NFS signal are typical features of the single resonance solution [6]. They originate from multiple nuclear scattering (see, e.g., [5,13] for a more detailed discussion).

In practice, however, a single resonance is not easy to realize. Hyperfine interactions and motion are always present to a certain extent. It is only the question of how small their influence is and how well the single resonance approximation describes the present case. An apparent single resonance spectrum is thus always a test of the low-frequency resolution limit of the spectroscopy technique in use.

The length of the time interval in which one can measure the nuclear decay defines the low-frequency resolution limit in time-domain spectroscopy. The wider the time window, the finer the details of the nuclear resonance that can be resolved. The only limiting factor is the statistical accuracy of measurements (number of counts per channel). This statement is demonstrated by the example of the 14.4 keV resonance in ^{57}Fe nuclei in stainless steel.

From Mössbauer spectroscopy in the energy domain it is well known that ^{57}Fe nuclei in stainless steel reveal an apparent single nuclear resonance with a small additional broadening of about $1\Gamma_0$. To resolve its fine structure and thus to understand the nature of the broadening is difficult with a Mössbauer source because it has an energy width of about the same magnitude. To the knowledge of the author the nature of the broadening in stainless steel is not yet fully understood. Let us see if by time spectroscopy we can gain more insight into this problem.

Stainless steel foils of the composition $Fe_{55}Cr_{25}Ni_{20}$, enriched to 95% in ^{57}Fe, were used in the studies reported. Mössbauer energy spectra measured with one of

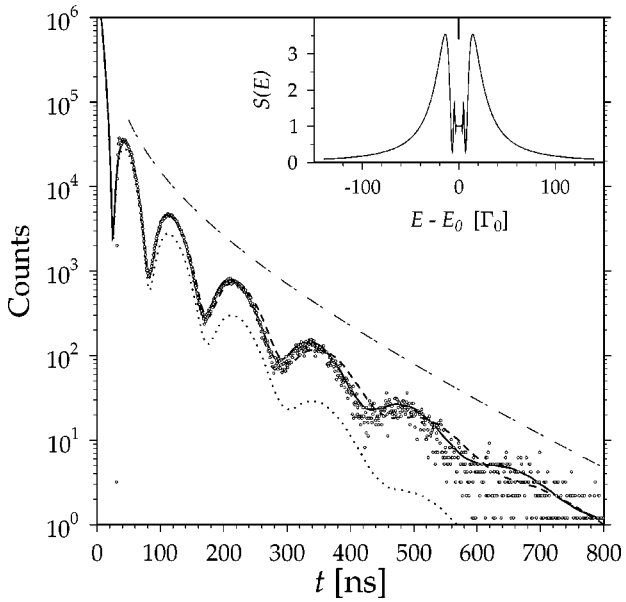

Figure 1. Time spectrum of nuclear forward scattering from a stainless steel foil $\simeq 12$ μm thick. The lines are fits with MOTIF. The effective nuclear resonance thickness was averaged in the range $T'_{\rm R} = 85 \pm 11$. The dashed line is a simulation of the NFS time spectrum with an unbroadened single resonance. Dotted line: single resonance with an additional Lorentzian broadening of $\Delta\Gamma_0 = 0.62\Gamma_0$. Solid line: NFS time spectrum calculated with the same Lorentzian broadening; however, truncated beyond the bounds of $\pm 2\Gamma_0$. The dashed-dotted line is $\propto \exp(-\Gamma_0 t)/t^{3/2}$, which approximates the average decay rate of the resonant nuclear ensemble in the forward direction for $t \geqslant 50$ ns [6]. The inset shows the energy spectrum of NFS (corresponding to the solid-line time spectrum) with a double-hump structure typical for a thick single resonance scatterer.

these samples with the help of CEMS[3] have shown an additional line broadening of $0.62\Gamma_0$.

The time spectra of NFS measured in a time window of 700 ns in foils of different thicknesses, measured by the author at HASYLAB/F4, are shown in [13, figure 2]. The time spectrum of NFS of a sample of the same origin measured by the Nuclear Diffraction Group (ESRF) at ID18/ESRF [14] with improved statistics is shown in figure 1. The spectrum was measured in 4.6 h in a time window of 0.04–2.7 μs in the single bunch mode of the ESRF storage ring with an average current of 10 mA. To exclude any possible influence of nuclear resonance small-angle scattering [4] on the NFS time spectrum a Si(1 1 1) channel-cut crystal analyser was installed downstream of the foil. We shall discuss the evaluation of this spectrum in some detail.

[3] Conversion electron Mössbauer spectroscopy (CEMS) measurements performed by Eva Giesse, Universität Erlangen, and Olaf Leupold, Universität Hamburg, have shown that the line width of the nuclear resonance in our stainless steel samples is 0.06 mm/s broader than in a sample of α-Fe, believed to have unbroadened lines. I.e., the resonance width in our samples of stainless steel is 62% broader than the natural width of the 14.4 keV resonance in ^{57}Fe nuclei, which is equal to 0.097 mm/s.

The spectrum reveals dynamic beats. The response is speeded-up and follows on the average the $\exp(-\Gamma_0 t)/t^{3/2}$ time dependence [6]. Both effects are due to coherent multiple resonance scattering taking place in thick samples.

The dashed line is the time spectrum calculated by MOTIF for a single resonance of natural width Γ_0. The dotted line shows the time spectrum calculated with an additional Lorentzian broadening of $\Delta\Gamma_0 = 0.62\Gamma_0$, as in eqs. (3.2)–(3.3). Surprisingly, the additional broadening as suggested by the measured CEMS Mössbauer spectrum, gives a much worse fit.

Another model was tested: the additional broadening is assumed to be due to a small magnetic splitting caused by a weak magnetic hyperfine field at the nuclear sites (the case with a large magnetic splitting is discussed in section 3.1.2). E.g., a field of $B = 0.2$ T should produce the required broadening of $0.6\Gamma_0$. However, the time spectrum evaluated with such a magnetic field shows practically no difference from that calculated for a true single line (dashed line). But the time spectrum calculated with a field of 0.52 T fits very well to the experimental data (solid line). However, the CEMS energy spectrum calculated with such a magnetic field gives a double-peak structure with $3\Gamma_0$ total width and this seems to discard this model.

One more model was tested, based on the fact that stainless steel is an unordered alloy with a finite number of nonequivalent nuclear sites. In these sites the nuclear resonance may experience different isomer (chemical) shifts. The distribution of the isomer shifts, however, should be limited. The solid line in figure 3 is the time spectrum evaluated for a set of single resonance lines with a Lorentzian distribution of isomer shifts. This distribution was $0.6\Gamma_0$ broad, but it was truncated beyond the bounds $\pm 2\Gamma_0$. Such a bounded distribution gives both the required broadening in the CEMS energy spectrum and the time spectrum which fits well the experimental points. Thus the model of the bounded isomer shift distribution gives predictions which agree both with the results obtained by the time- and energy-domain nuclear resonance spectroscopies.

This example demonstrates that there is no "better" spectroscopic technique. The complementary information supplied by both energy- and time-domain techniques helps to find the best model.

3.1.2. Magnetic splitting

The evaluation of the NFS time spectrum in a nuclear system with magnetically split sublevels in the ground and excited states is presented in this section. The nuclear ensemble consists of ^{57}Fe nuclei in a ferromagnetic α-Fe foil.

The time spectrum shown in figure 2 was measured with a 1 μm thick α-Fe foil enriched to 95% in ^{57}Fe. The measurements were performed at F4/HASYLAB [12]. The foil was magnetized by a magnetic field applied in the plane of the foil and perpendicular to the synchrotron radiation beam so that only the two $m_{\rm e} - m_{\rm g} = \Delta m = 0$ nuclear transitions were excited. Here $m_{\rm e}, m_{\rm g}$ are the magnetic quantum numbers in the nuclear excited and ground states, respectively. The interference of the two different monochromatic components originating from the two excited nuclear transitions

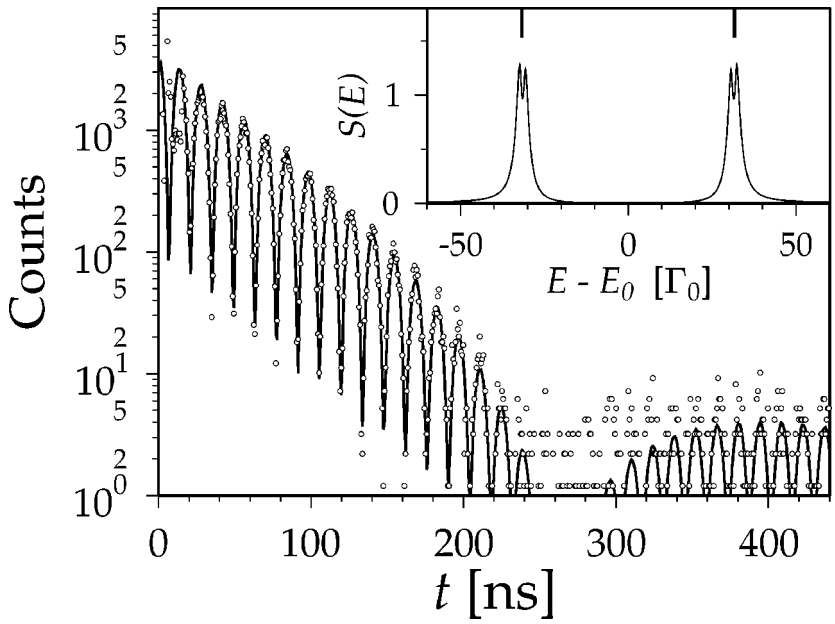

Figure 2. Measured (circles) and MOTIF-fitted (solid lines) NFS time spectra from a 1 μm thick magnetized α-Fe foil with $\Delta m = \pm 1$ transitions excited [12]. The corresponding calculated energy spectrum of NFS is shown in the inset. The positions of the excited nuclear transitions are marked by the vertical lines in the upper part of the inset.

(the vertical lines in the inset of figure 2) leads in the time spectrum to the periodic modulation called quantum beat [1,7]. The two excited transitions yield a quantum beat with a single period of $2\pi\hbar/\delta E$, which is defined by their separation $\delta E = 63.3\Gamma_0$. Because of the large sample thickness ($T'_{\rm R} = 7.8$), the initial decay is about three times faster than natural and the first minimum of the dynamical beat occurs at $\simeq$270 ns. The solid line is the fit with MOTIF. The inset in figure 2 shows the corresponding calculated energy spectrum of NFS with the characteristic double-hump structure.

The time spectrum in figure 3 (open circles) was measured with a thicker α-Fe foil of 10.6 μm thickness of the same enrichment. In this case the foil was magnetized in such a way that another four, in this case $\Delta m = \pm 1$, nuclear transitions were excited (as before, an external magnetic field is applied in the plane of the foil and perpendicular to the synchrotron radiation beam). The measurements were performed by the Nuclear Resonance Group (ESRF) at ID18/ESRF [14]. The spectrum in figure 3 was measured for 9.5 h in the time window 0.04–2.7 μs in the single bunch mode of the ESRF storage ring with an average current of 10 mA. To exclude any influence of nuclear resonance small-angle scattering [4] on the time spectrum a Si(1 1 1) channel-cut crystal analyser was installed downstream of the Fe foil.

The solid line in figure 3 shows the fit of the time spectrum with MOTIF by using expressions (3.2)–(3.3) for the nuclear self-correlation function and the multiple scattering (2.2)–(2.4). One nuclear site was used ($\beta = 1$) with $\langle\beta_\lambda| = \langle m_\lambda|$ and

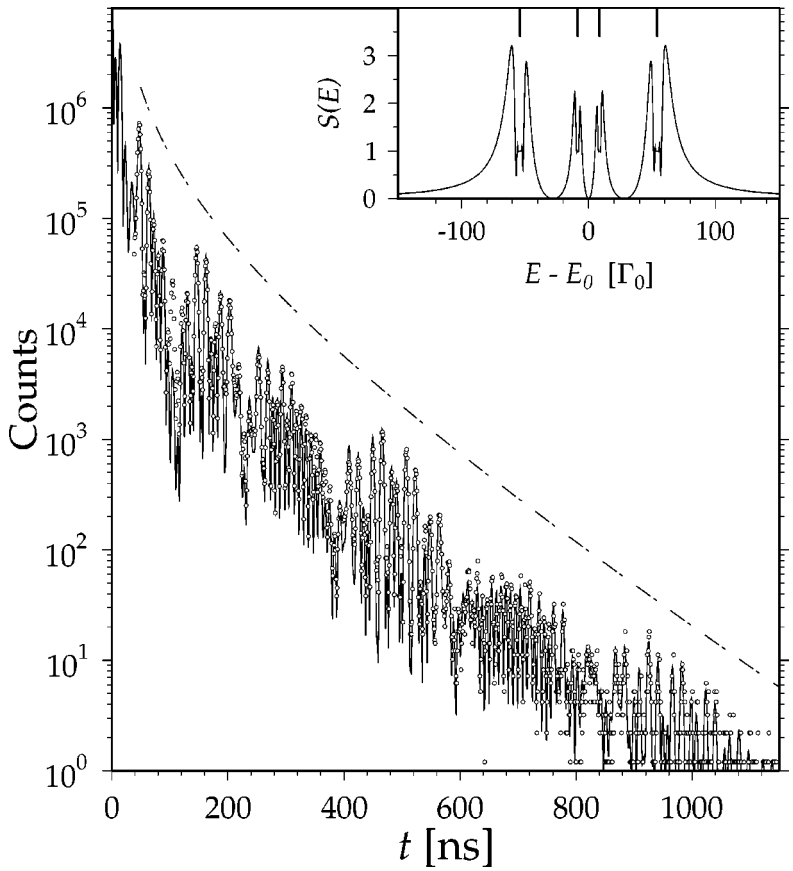

Figure 3. Time spectrum of nuclear forward scattering from a magnetized α-Fe foil $\simeq$10.6 μm thick with $\Delta m = \pm 1$ transitions excited. The solid line is the fit with MOTIF. The dashed-dotted line is $\propto \exp(-\Gamma_0 t)/t^{3/2}$, which approximates the average decay rate of the resonant nuclear ensemble in the forward direction for $t \geqslant 50$ ns [6]. The corresponding calculated energy spectrum of NFS with a double-hump structure which is typical for thick samples is shown in the inset. The positions of the excited nuclear transitions are marked by the vertical lines in the upper part of the inset.

$\varepsilon_{m_\lambda} = -\mu_\lambda m_\lambda B/J_\lambda$. Here μ_λ are the nuclear magnetic moments and B is the magnetic hyperfine field at the nuclear site.

The fit procedure yielded an effective thickness $T'_{\rm R} = 174 \pm 16$. The value ± 16 gives the range of averaging of the time spectrum over the inhomogeneous sample thickness resulting from the fit. Multiple scattering events of up to 40th order contribute to the NFS spectrum of the sample with such an effective thickness and in the 1200 ns time window of evaluation. In other words, 40 terms in the sum of eq. (2.2) must be taken into account to calculate such a spectrum.[4] The agreement between the calculated and the measured time spectra is nearly perfect in the time window,

[4] The calculation time for such a spectrum is $\simeq$5 s with MOTIF.27 running under LINUX by using a 100 MHz 486PC with 32 MB RAM.

which is as large as 8.2 natural lifetimes $\tau_0 = \hbar/\Gamma_0 = 141.1$ ns of the 14.4 keV excited state of ^{57}Fe nuclei and in the count rate range which spreads over 6 orders of magnitude.

The fit procedure, which runs automatically, allows one to obtain the values of the magnetic field B at the nuclear site and the ratio μ_e/μ_g of the nuclear magnetic moments in the excited and ground states with a relative accuracy of 30 ppm. With the magnetic moment in the ground state, $\mu_g = 0.09044(7)\,\mu_N$ [15], the field was found to be $B = 32.623(1)$ T. The ratio of the nuclear magnetic moments was found to be $\mu_e/\mu_g = -1.71105(6)$. For comparison, the values of the ratio given by other authors are: $\mu_e/\mu_g = -1.7127(6)$ [15] and $\mu_e/\mu_g = -1.7142(4)$ [16].

The apparent quantum beat frequency arises in the first place from the frequency difference of the outer nuclear transitions. However, the frequency and beat amplitude are not constant. The envelope of the beat amplitude and the modulation of the beat frequency originate from the combined influence of the multiple scattering effects in thick samples and the presence of another two inner nuclear transitions. For comparison, the time spectrum of a much thinner α-Fe foil, measured under very similar conditions, as presented in [12,17], shows a very different envelope and frequency modulation.

Other examples of using MOTIF for evaluation and fitting of NFS time spectra under conditions of time-independent hyperfine interactions are presented, e.g., in [12, 13,17,18].

3.1.3. Distribution of the hyperfine parameters

Nuclear resonance spectra measured in alloys, amorphous materials, etc., often reveal variation of magnetic hyperfine fields, electric field gradients, and isomer shifts, which the resonant nuclei experience in different sites. This situation can be fairly well described by introducing distributions of the hyperfine parameters. The distribution of the isomer shifts was already used in the evaluation of the time spectrum in stainless steel in section 3.1.1. The following example, in figure 4, demonstrates how the magnetic field distribution can be used to evaluate with MOTIF NFS time spectra in magnetic alloys. At this point it is helpful to recollect for contrast the time spectrum shown in figure 2, from a nuclear ensemble experiencing equal magnetic hyperfine fields at all nuclear sites.

An invar alloy of composition $Fe_{65}Ni_{35}$, enriched to 95% in ^{57}Fe, was used as a sample material with a static magnetic hyperfine field distribution. The time evolution of NFS by an invar foil of thickness 1.2 μm placed in a vertical magnetic field [12] is shown in figure 4. Only the two transitions with $\Delta m = 0$ were excited. The effective resonance thickness $T'_R = 5.6$ of the invar foil is slightly less than that of the iron foil in figure 2. Although the effective thickness is less the decay of the NFS signal is much faster. It is approximately exponential with a decay constant $6.5\tau_0$. The reason for such a fast decay is the inhomogeneous broadening of the nuclear resonance due to the distribution of magnetic hyperfine fields at nuclear sites. The appropriate distribution was modelled by the superposition of three Gaussians. The distribution

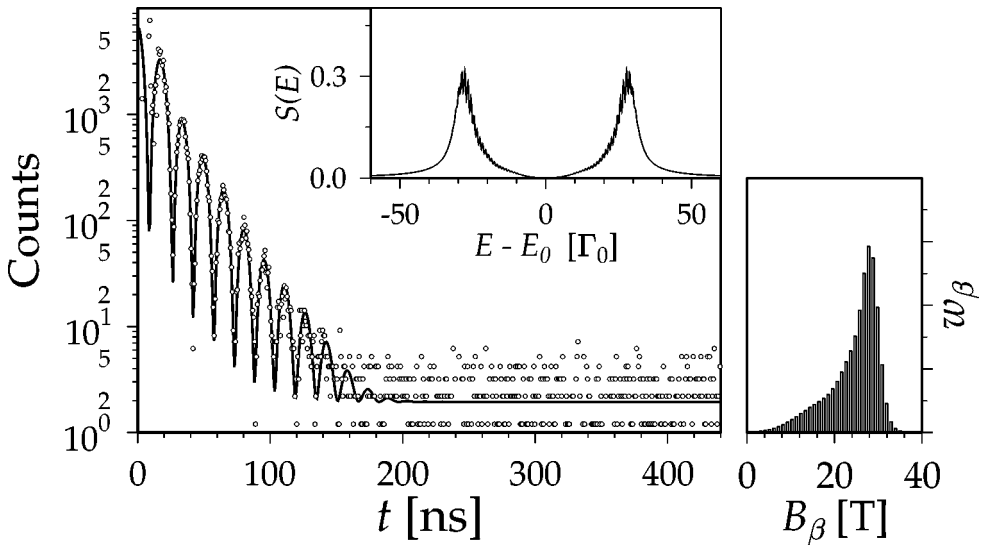

Figure 4. Measured (circles) and MOTIF-fitted (solid lines) NFS time spectra from a 1.2 μm thick magnetized invar foil with $\Delta m = \pm 1$ transitions excited [12]. The corresponding calculated energy spectrum of NFS is shown in the inset. The graph on the right shows the distribution of the magnetic hyperfine fields used to fit the time spectrum.

used to fit the time spectrum is shown on the graph to the right. The distribution is asymmetric. By using this distribution profile it was possible to fit time spectra of samples with different thicknesses [12]. The asymmetric distribution leads to hybrid beat phenomena, as discussed in [12,17].

3.2. Magnetic hyperfine field switching

As was argued in section 1, the method of direct calculation in time as used in MOTIF is especially attractive if the frequency spectrum of NFS is not known or not easily calculated. This is the case of time-dependent hyperfine interactions, e.g., caused by external perturbation. If the perturbations are synchronized with the time of nuclear excitation, they will result in *inelastic coherent* scattering, and thus will allow one to manipulate the spectrum, the intensity, and the polarization state of the reemitted radiation. Effects of manipulation of the coherent radiation caused by an instantaneous switching of the magnetic hyperfine field were extensively studied during the last decade (see, e.g., [19] and references therein). The fast switching of the hyperfine field was accomplished by abruptly changing the direction of the external magnetic field.

In the formal language of the NFS theory [5], switching of the magnetic hyperfine field direction means switching between different nuclear self-correlation functions. Indeed, as is easy to realize, before switching the directions of the hyperfine fields are constant, the hyperfine interactions are time-independent and the self-correlation function of the nuclear ensemble is given by eqs. (3.2)–(3.3). After instantaneously

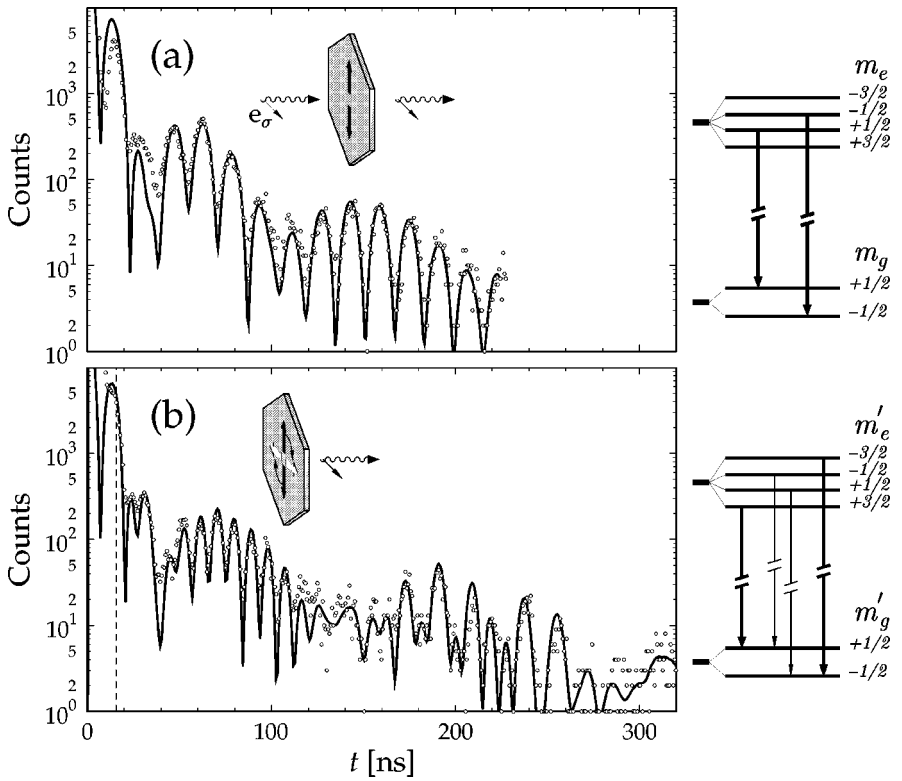

Figure 5. Measured (circles) and MOTIF-fitted (solid lines) NFS time spectra from a $^{57}FeBO_3$ single crystal (a) with constant direction of the hyperfine fields, as indicated in the figure; and (b) with the magnetic hyperfine fields rotated by 90° in the easy magnetization plane of the $^{57}FeBO_3$ crystal at $t' = 18$ ns after excitation by the synchrotron radiation pulse [19]. The attached schemes of nuclear energy levels show the transitions at which the nuclei radiate after their excitation (a) and the transitions at which they radiate after switching (b).

changing the magnetic hyperfine field directions at each nucleus in the ensemble, at $t = t'$, the hyperfine interactions are again time-independent. The nuclear self-correlation function is formally given by the same expression (3.2)–(3.3), however, with new transition frequencies $\Omega_{\ell'}$, and different amplitudes $\mathcal{A}_{\ell'}(\chi, t' - \tilde{t})$. As before, the amplitudes of the new transitions ℓ' are (cf. eq. (3.4)) products of the excitation and de-excitation transition currents; however, the excitation currents are now a coherent linear superposition of the initially excited transition currents. The coefficients which define this superposition depend on the angle of switching χ and the time difference $t' - \tilde{t}$ between excitation at $\tilde{t}$ and switching at t', cf. [5, eqs. (84)–(86)]. This gives the possibility to manipulate the coherent radiation in a deliberate way by a proper choice of switching angle and switching time.

Figure 5 shows an example of switching from the $\Delta m = 0$ to the $\Delta m = \pm 1$ spectrum with the help of an instantaneous 90° rotation of the magnetic hyperfine field direction at the nuclei. The measurements of the NFS time spectrum from a $^{57}FeBO_3$

single crystal and the evaluation with MOTIF are shown (a) without switching and (b) with a 90°-rotation of the magnetic hyperfine fields in the easy magnetization plane at $t' = 18$ ns after excitation by the synchrotron radiation pulse [19]. Without switching – figure 5(a) – or before switching – figure 5(b) – for $t < 18$ ns the nuclear system radiates with the $\Delta m = 0$ transitions. Abrupt 90°-switching forces the nuclear system to radiate with the $\Delta m' = \pm 1$ transitions, as shown in the nuclear transition schemes of figure 5. This leads to a different NFS time spectrum, which resembles the "usual" $\Delta m = \pm 1$ time spectrum as shown, e.g., in figure 3. The use of primed magnetic quantum numbers m' is due to the new quantum axis after switching.

Further examples for the influence of the magnetic hyperfine field switching on the NFS time spectra and the results of their evaluation with MOTIF are given in [19].

3.3. Diffusion

The influence of the diffusive motion of the nuclei on the NFS time spectra is described with the help of the motional part of the nuclear self-correlation function $M_\beta(t, \tilde{t})$. Actually $M_\beta(t, \tilde{t})$ contains all forms of motion and not only diffusion. However, if a diffusion process can be thought of as independent of the thermal vibrations, etc., then $M_\beta(t, \tilde{t})$ factorizes with the diffusional self-correlation function as an independent factor. As diffusion does not correlate with the time instants of photon absorption or emission, only its elastic part contributes to the coherent NFS scattering. Therefore, in this case $M_\beta(t, \tilde{t}) = \mathcal{M}_\beta(t - \tilde{t})$. The self-correlation functions for different models of diffusion, e.g., continuous free diffusion [21], continuous localized diffusion [22], and free jump diffusion [23] have the same form:

$$\mathcal{M}(t) = \sum_\alpha a_\alpha \exp\left(-\frac{\gamma_\alpha}{2\hbar} t\right). \tag{3.6}$$

The physical meaning of the coefficients a_α, γ_α depends on the model. Different diffusion models in connection with NFS were recently reviewed in [9].

Mathematically the diffusion self-correlation functions (3.6) and that of the time-independent hyperfine interactions (3.2) are equivalent. Thus, the same version of MOTIF can also be applied for evaluations of the NFS time spectra influenced by diffusive motions of nuclei.

3.4. Relaxation

Since the spins of atoms to which resonant nuclei belong fluctuate in time, the hyperfine interactions, as seen by the nuclei, are generally speaking time dependent. This time dependence reveals itself in the nuclear resonance time and energy spectra provided the fluctuation (relaxation) times are comparable with the nuclear lifetime. To describe time spectra influenced by relaxation effects is a complicated problem. However, the method which is implemented in MOTIF allows us to handle such a problem formally in the same way as all other cases described previously. The same

rule is valid here: define the self-correlation function of the problem, and for the rest apply the standard multiple scattering procedure. Thus the problem of evaluation of the NFS time spectra in the presence of atomic spin relaxation is the problem of evaluation of the corresponding nuclear self-correlation function.

As has been pointed out already in the very first theoretical paper [24] in which the influence of atomic spin relaxation on the hyperfine structure of the nuclear resonance was discussed, the time correlation function is given by an expression mathematically equivalent to eq. (3.2). However, in this case the space of nuclear eigenstates $|\beta\rangle$ should be extended to the unified space of the eigenstates of atomic and nuclear spins. The summation in eq. (3.2) should thus be performed not only over the nuclear variables, but over electron spin variables as well.

4. How to obtain the program?

Executable files of MOTIF precompiled on different Unix platforms are available from the anonymous `ftp://i2aix04.desy.de/pub/motif/` as part of a distribution package. The newest and also previous versions of MOTIF are available. Different versions and their distribution packages are distinguishable through appended numbers, like MOTIF.23, MOTIF.27, etc.

The distribution package of each version also contains a detailed User's Guide supplied as a file MOTIF_VERSION.PS in postscript format. In subdirectories of the distribution also examples for fitting real time spectra are provided.

Acknowledgements

The author is indebted to Erich Gerdau for supporting this work, to Walter Potzel for very many fruitful discussions, for many suggestions of improving MOTIF's functionality, and for testing MOTIF during many years, to Alexander Chumakov for putting the data sets of the measured time spectra of α-Fe and stainless steel foils at the author's disposal. The author further thanks Uwe van Bürck, Hans Dierk Rüter, and Alexander Chumakov for helpful discussions and remarks after reading the manuscript. The work was supported by the Bundesministerium für Bildung, Forschung und Technologie under Contract No. 05 643GUA1.

References

[1] E. Gerdau, R. Rüffer, R. Hollatz and J.P. Hannon, Phys. Rev. Lett. 57 (1986) 1141.
[2] J.B. Hastings, D.P. Siddons, U. van Bürck, R. Hollatz and U. Bergmann, Phys. Rev. Lett. 66 (1991) 770.
[3] R. Röhlsberger, this issue, section III-1.4.
[4] Yu.V. Shvyd'ko, A.I. Chumakov, A.R.Q. Baron, E. Gerdau, R. Rüffer, A. Bernhard and J. Metge, Phys. Rev. B 54 (1996) 14942.
[5] Yu.V. Shvyd'ko, Phys. Rev. B 59 (1999) 9132; also this issue, section III-1.3.

[6] Yu. Kagan, A.M. Afanas'ev and V.G. Kohn, J. Phys. C 12 (1979) 615.
[7] G.T. Trammell and J.P. Hannon, Phys. Rev. B 18 (1978) 165; ibid 19 (1979) 3835.
[8] W. Sturhahn and E. Gerdau, Phys. Rev. B 49 (1994) 9285.
[9] G.V. Smirnov and V.G. Kohn, Phys. Rev. B 52 (1995) 3356;
V.G. Kohn and G.V. Smirnov, Phys. Rev. B 57 (1998) 5788.
[10] L. Deák, L. Bottyàn, D.L. Nagy and H. Spiering, Phys. Rev. B 53 (1996) 6158.
[11] M. Haas, E. Realo, H. Winkler, W. Meyer-Klaucke, A.X. Trautwein, O. Leupold and H.D. Rüter, Phys. Rev. B 56 (1997) 14082.
[12] Yu.V. Shvyd'ko, U. van Bürck, W. Potzel, P. Schindelmann, E. Gerdau, O. Leupold, J. Metge, H.D. Rüter and G.V. Smirnov, Phys. Rev. B 57 (1998) 3552.
[13] U. van Bürck, this issue, section IV-2.1.
[14] R. Rüffer and A.I. Chumakov, Hyp. Interact. 97/98 (1996) 589.
[15] A = 57^{*}, Nuclear Data Sheets 67 (1992) 195.
[16] J.G. Stevens and V.E. Stevens, *Mössbauer Effect Data Index Covering the 1975 Literature* (IFI/Plenum, New York/Washington/London, 1976).
[17] Yu.V. Shvyd'ko and U. van Bürck, this issue, section IV-2.2.
[18] R. Lübbers, G. Wortmann and H.F. Grünsteudel, this issue, section IV-2.3.
[19] Yu.V. Shvyd'ko, T. Hertrich, U. van Bürck, E. Gerdau, O. Leupold, J. Metge, H.D. Rüter, S. Schwendy, G.V. Smirnov, W. Potzel and P. Schindelmann, Phys. Rev. Lett. 77 (1996) 3232.
[20] Yu.V. Shvyd'ko, A.I. Chumakov, G.V. Smirnov, V.G. Kohn, T. Hertrich, U. van Bürck, E. Gerdau, H.D. Rüter, J. Metge and O. Leupold, Europhys. Lett. 22 (1993) 305.
[21] K.S. Singwi and A. Sjölander, Phys. Rev. 120 (1960) 1093.
[22] A.M. Afanas'ev and V.E. Sedov, Phys. Status Solidi B 131 (1985) 299.
[23] O.G. Randl, B. Sepiol, G. Vogl, R. Feldwisch and K. Schroeder, Phys. Rev. B 49 (1994) 8768.
[24] A.M. Afanas'ev and Yu. Kagan, Soviet Phys. JETP 18 (1963) 1139.